Vol. 04, Iss. 1 (2026) 1-9, DOI: 10.61552/JME.2026.01.001

JME

Journal of Materials and Engineering

www.jme.aspur.rs

Research article

Improving the Performance of FeCrAl Coatings: A Microstructural and Mechanical Perspective

Bauyrzhan Rakhadilov[a], Aidar Kengesbekov[b,c], Umar Ibtasam[a,b,*], Magazov Nurtoleu[c]

[a]*PlasmaScience LLP, Ust-Kamenogorsk, Kazakhstan.*
[b]*Institute of composite materials, Ust-Kamenogorsk, Kazakhstan.*
[c]*D. Serikbayev East Kazakhstan Technical University, Ust-Kamenogorsk, Kazakhstan.*

Keywords:

FeCrAl coatings
XRD
Plasma spraying
Coating uniformity
Wear resistance
Micro hardness
Surface analysis

* Corresponding author:

Umar Ibtasam
E-mail: ibtasamumar@gmail.com

Received: 6 March 2025
Revised: 26 April 2025
Accepted: 6 June 2025

A B S T R A C T

In this study explores the properties and performance of FeCrAl coatings applied to steel substrates, focusing on thickness, hardness, and surface roughness. The coating thickness varied between 215.95 µm and 270.35 µm across the samples. Hardness measurements consistently averaged around 94 HRB, indicating that thickness had minimal impact on this property. Surface roughness analysis revealed a decreasing trend with increasing coating thickness, attributed to enhanced uniformity in deposition. These results underscore the critical role of optimizing deposition parameters and surface preparation techniques to produce uniform FeCrAl coatings with reliable mechanical characteristics.

© 2026 Journal of Materials and Engineering

1. INTRODUCTION

The Introduction Advancements in surface engineering have led to the development of coatings that significantly enhance the performance and durability of materials used in demanding industrial applications. Parameters of microstructure, fatigue strength, wear rate, corrosion resistance, coating porosity, hardness, toughness, deposition efficiency - DE, adhesive strength, surface roughness-SR, and oxide contents stand as the greatest in determining coatings characteristics [1]. Arc spraying is widely applied for protection of steel materials and re manufacturing of worn parts with the purpose of increasing their service life. It is preferred from other thermal spraying techniques, for example plasma spraying, because it has a higher deposition

efficiency, easier operation, and relatively cheaper equipment [2-3]. FeCrAl alloys are widely used as high temperature corrosion-resistant materials [4]. Fe-based alloys are one of the best candidates since it has excellent formability, with high strength and good resistance to oxidation at elevated temperatures. Oxidation kinetics and mechanisms for these high temperature applications of FeCrAl alloys have been investigated over a very wide range of temperatures and environments [5-13].

Generally speaking, the performance of FeCrAl coating is sensitive to the content of Cr and Al during service conditions [14]. FeCrAl composite coatings were deposited by atmosphere plasma spraying technique. The microstructure and the dielectric properties of composite coatings are reported, and possible mechanisms are discussed. Theoretical calculation of the microwave reflectivity coefficients of the coatings is conducted using permittivity of composite coatings with different fractions and thick-nesses [15].

FeCrAl coatings are highly valued for their very good resistance against oxidation, corrosion, and wear and thus are suitable for protection against extremely harsh environments like high temperature and corrosive media.

Properties of such coatings will depend on their microstructural and mechanical characteristics, including coating thickness, surface roughness, and hardness, responsible for durability, adhesion, and mechanical stress resistance. It is still challenging to achieve FeCrAl coating uniformity due to deposition processes, surface preparations, and environmental inconsistencies. In this work, the properties of coatings depending on these factors, such as thickness, hardness, and surface roughness, have been analyzed; then, causes for inconsistencies are identified and strategies for optimization, which refers to standardization at deposition techniques and improvement of surface preparation. Findings enhance the reliability and efficiency of FeCrAl coatings towards better practices in surface engineering for demanding industrial applications.

2. MATERIALS AND METHODS

Materials Substrate: Steel 200X13 was employed as the substrate material for the FeCrAl coatings. Coating Material: FeCrAl alloy powder was used as the feedstock for the coating deposition process. The specific composition of the FeCrAl alloy powder should be specified (e.g., Fe-25Cr-5Al, Fe-28Cr-4Al).

2.1 Coating Deposition Coating Process

FeCrAl coatings were deposited onto the steel substrates using plasma spraying. The coating process parameters, including key parameters, spray distance, powder feed rate, gas flow rates, were maintained constant throughout the deposition process. Different applications of sprayed coatings are growing steadily. Provide details of the coating equipment used. Coating deposition was performed using a spraying equipment system [16].

2.2 Sample Mounting

Samples were mounted using a Hot Mounting Press Machine Machine [17] with black polymer material for secure handling and improved grip during subsequent preparation steps.

2.3 Grinding Process

Grinding was performed with Alpha 200 Manual Polishing Machine [18] using progressively finer grit silicon carbide (SiC) papers (e.g., 120, 240, 400, 600, 800, 1000, 1200, 1500, 2000 & 2500 grit [19]. Polishing was carried out using diamond polishing suspensions with decreasing particle sizes (e.g., 3 μm, 1 μm, 0.25 μm) on polishing cloths. The final polishing step aimed to achieve a mirror like finish for accurate microstructural and surface roughness measurements.

2.4 Surface Finishing

The surface finishing treatments of the mounted samples were carried out by polishing with a MIRKA 5424105018 abrasive combined with Silica Sus-pension (OPS) [20] on a grinding polishing machine up to attaining a smooth, refined surface.

2.5 Characterization Coating Thickness Measurement

Coating thickness was measured using cross sectional microscopy, a high-accuracy technique for examining layered structures. The samples were mounted, ground, and polished with care to create a smooth, mirror-like cross-section for

measurement. A high-magnification optical microscope (20x magnification) was used to capture close-up photographs of the coating layers. To present representative data, measurements in thickness were taken at multiple locations on every sample.

2.6 Hardness Testing

Micro hardness measurements were performed using a Rock-well hardness tester [21]. The Rockwell hardness scale used was HRB. Multiple indentations were made on each sample, and the average hardness value was calculated.

2.7 Surface Roughness Analysis

Surface Roughness Analysis: using iSurfa-310 Roughness Waviness Tester [22] Surface roughness parameters, including Ra (average roughness), Rq (root mean square roughness), Rz (maximum peak-to-valley height), and Rt (total height), were measured using a Surface Roughness Machine. Measurements were taken over a specified scan length and number of scans per sample.

2.8 XRD Analysis

XRD Analysis: Using X-ray Diffractometers [23] FeCrAl coatings are composed of metallic, alloyed, and oxide phases that form during melting, solidification, and oxidation in the plasma spraying process. The formation of phases in these coatings is affected by high temperatures and rapid cooling; substrate temperature, spray distance, and feedstock flow rate have great influences on coating microstructure.

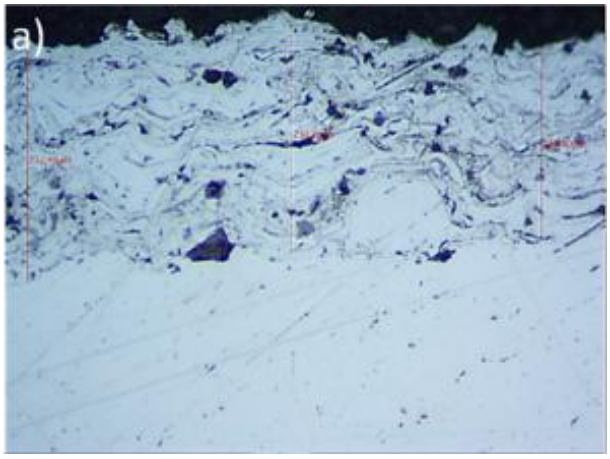
2.9 Coefficient of friction Analysis

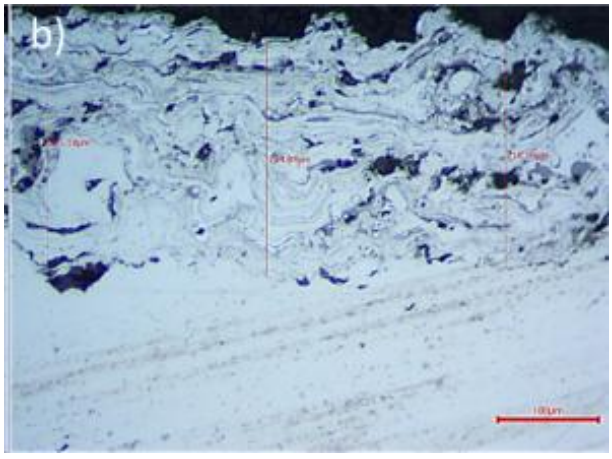
Using Pin-on-disk tribometer [24] The frictional behaviour of four FeCrAl samples was investigated using a TRB3 Tribometer under controlled conditions: 4.00 N normal load, 6.00 cm/s sliding speed, and 3.00 mm sliding radius to ensure uniform wear paths.

3. RESULTS & DISCUSSION

3.1 Coating Thickness

The FeCrAl coatings exhibited large difference variations in thickness across the analyzed samples, with measured values of 215.95 μm, 226.08 μm, 266.47 μm, and 270.35 μm for Samples 1, 2, 3, and 4, respectively (Fig 1). This result illustrates that there is a big difference among them, where Sample 4 showed the highest value for thickness and Sample 1 the lowest. Besides, it is important to say that the variation percentage was 25%, with a difference in thickness of 54.39 μm. Such variability suggests that there were inconsistencies in the coating deposition process, possibly arising from plasma spray parameters, substrate surface preparation, and thermal gradients during preheating. Variations in spray distance, feed rate, and nozzle alignment, as well as inconsistencies in sandblasting and substrate cleanliness, could contribute to the observed differences. Additionally, any non-uniform substrate preheating could led to localized variations in adhesion and thickness uniformity. By Statistically analyzing the results, the thickness measurement gave an average value of about 244.71 μm with a standard deviation of 24.14 μm, again showing that much remains to be done to improve the process.





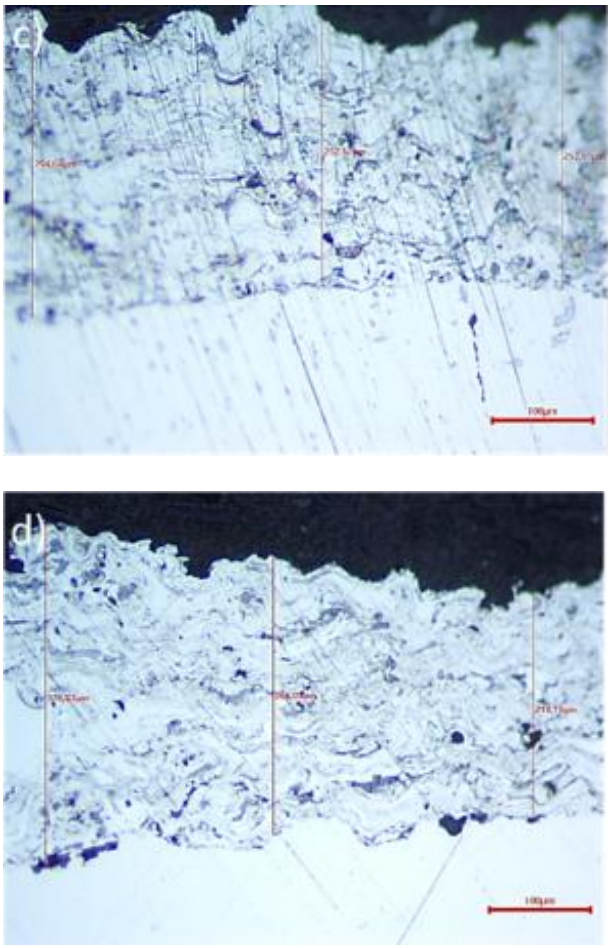


Fig. 1. Coating Thickness of FeCrAl samples.

Again, the improvement in plasma-spraying parameters, substrate preparation procedure, and online control should be considered in view of coating thickness to provide uniform thickness and homogenous mechanical properties. In the future, optimization should take environmental factors like temperature and humidity into consideration to allow more consistent deposition and a better quality coating.

3.2 Rockwell Hardness

Measurements The hardness values measured using the Rockwell Hardness Scale B (HRB) were relatively consistent across all samples, suggesting that the coating material and deposition process did not significantly influence hardness (Fig 2). The HRB values obtained were: Sample 1: 94 HRB Sample 2: 95 HRB Sample 3: 93 HRB Sample 4: 94.5 HRB These hardness values are quite close to each other, falling within a narrow range of 93–95 HRB. Despite the significant variation in coating thickness, hardness did not correlate directly with thickness. This finding suggests that the hardness of the FeCrAl coating is largely determined by the material properties of the FeCrAl itself rather than the coating thickness. It is important to consider that the hardness may also be influenced by other factors such as residual stresses introduced during the coating process. Coating deposition techniques like plasma spraying can induce internal stresses, which could affect hardness without influencing the coating thickness. The uniformity in hardness suggests that FeCrAl coatings, when applied consistently, maintain similar mechanical properties across a range of thicknesses.

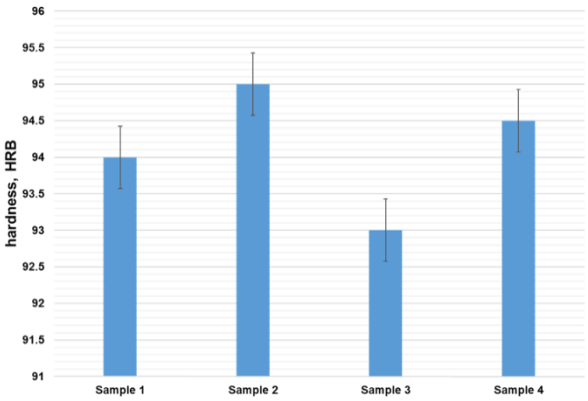


Fig. 2. Rockwell Hardness of FeCrAl samples

3.3 Surface Roughness

Surface roughness was measured using several parameters, including Ra (average roughness), Rq (root mean square roughness), Rz (maxi-mum peak-to-valley height), and Rt (total roughness height). The results for each sample are summarized in Table 1:

Table 1. Surface Roughness.

Samples	Surface Roughness Parameters			
	(Ra)	(Rq)	(Rz)	(l/min)
FrCrAl(1)	24.89 μm	31.154	162.087	195.23
FrCrAl(2)	27.22 μm	33.793	179.856	190.58
FrCrAl(3)	23.90 μm	29.671	146.665	155.37
FrCrAl(4)	22.98 μm	28.354	130.451	164.12

These parameters were chosen to analyze the effect of varying the voltages on the roughness results reveal an inverse relationship between coating thickness and surface roughness. As the

coating thickness increased from Sample 1 to Sample 4, the roughness parameters generally decreased (Fig 3). Notably, Sample 1, with the thin-nest coating, exhibited the highest roughness values, especially Ra (24.89 μm) and Rz (162.09 μm). In contrast, Sample 4, with the thickest coating, showed the lowest roughness values, with Ra measuring 22.98 μm and Rz measuring 130.45 μm. This trend suggests that thicker coatings, such as those applied to Samples 3 and 4, result in smoother surfaces. Thicker coatings are more likely to fill in the micro irregularities of the substrate and other surface imperfections, leading to a more uniform and smoother finish after polishing. The reduction in surface roughness could also be attributed to the more uniform deposition of the FeCrAl material in the case of thicker coatings. Additionally, improved polishing effectiveness and higher coating mass may contribute to the smoother surface observed in the thicker samples. Interestingly, Sample 2, despite having a coating thickness only slightly greater than Sample 1, exhibited the highest roughness parameters across all samples. This anomaly could suggest that the coating deposition process for Sample 2 was less uniform or that surface preparation prior to coating was less effective, resulting in more pronounced surface irregularities. It would be beneficial to further investigate the deposition parameters and surface preparation for this sample in future studies to ensure.

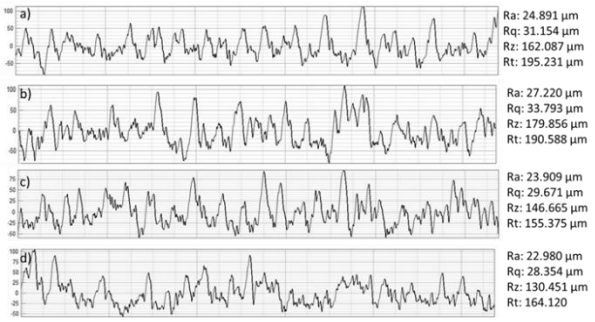


Fig. 3. Surface Roughness of FeCrAl samples.

3.4 X-Ray Diffraction

XRD analysis has given an insight into the phase composition of the FeCrAl coatings on all four samples: a variety of metallic, alloyed, and oxide phases that were formed in plasma spraying. High-energy conditions in plasma promoted complex physicochemical reactions, such as melting, rapid solidification, and oxidation of feedstock material. These phases are a result of the complex interaction among high temperature reactions, element diffusion, and dynamic cooling rates during deposition. The high temperatures in the plasma jet contributed to vaporization and even partial decomposition of the starting FeCrAl feedstock material; fast quenching upon impact with the substrate resulted in the crystallization of the different phases. More precisely, extremely high oxygen content in the plasma environment participated widely in incorporating oxide phases including but not limited to Wustite, Magnetite, and Chromium Oxide. Simultaneously, the retention of metallic aluminium, alloyed Chromferide, and Chromite disclose partial preservation of the feedstock from their natural composition and reveal chemical interaction across the coating to the steel substrate.

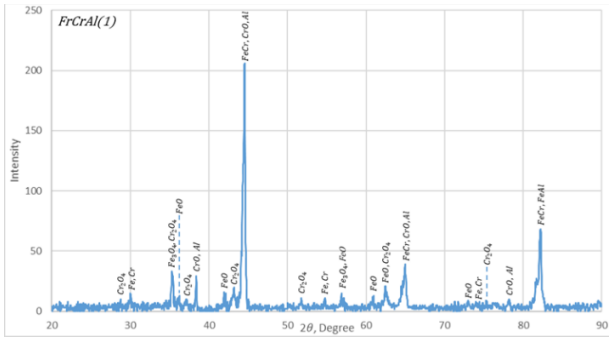


Fig. 4. XRD sample 01.

These results again point out that plasma spraying is a complex process, and even slight variations in substrate temperature, spray distance, and feedstock flow rate may cause considerable changes in the phase composition and microstructure of the coatings. Sample 1: The XRD pattern of Sample 1 (Fig 4) presented significant peaks for Aluminium Al, Chromium Oxide $CrO_{0.87}$, Chromferide Fe,Cr, Chromite $Fe^2Cr_2O_4$, Wustite $Fe_{0.9536}O$, and Magnetite Fe_3O_4. The diffraction peaks were in a wide two-theta range, from about 10° to 90°, reflecting a diverse phase composition due to the plasma spraying process. The presence of $CrO_{0.87}$ and Chromferide with chromium-based compounds indicates the interaction of chromium with both substrate and coating material during deposition. Besides, the strong presence of iron oxides, such as Wustite and Magnetite, signifies that there was an oxygen rich environment during the coating process, hence facilitating the oxidation of iron.

The peaks for Chromite $Fe^2Cr_2O_4$ show a good reaction between chromium with the iron from the steel substrate to form a spinel structure. These phases, in concert, suggest that in Sample 1, a balance between oxidation and alloy retention had been achieved with the deposition process, contributing to its complex microstructure.

Sample 2: Similar to Sample 1, the peaks identified in Sample 2 (Fig 5) are those of Al, $CrO_{0.87}$, Fe,Cr, $Fe^2Cr_2O_4$, $Fe_{0.9536}O$ and Fe_3O_4. However, a comparison between the two samples has shown a slight variation in peak intensities, hence showing that these phases were in relative fractions different from one sample to the other. Such differences are probably associated with slight variations in deposition parameters such as temperature differences or change in the feed rate of the deposited material. The slightly higher intensity of $CrO_{0.87}$ peaks in this Sample suggests that oxidation of chromium was more effective during deposition, probably because of higher exposure to oxygen within the plasma jet.

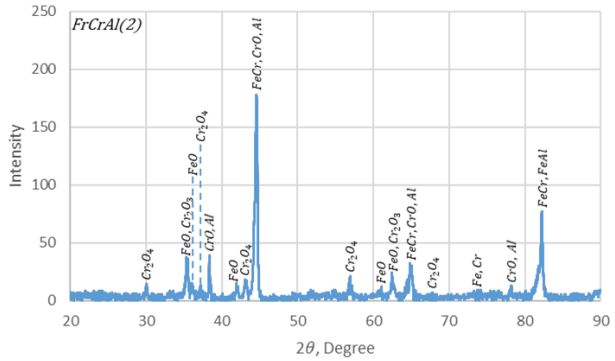


Fig. 5. XRD sample 02.

Besides, the higher Wustite formation compared to Magnetite might indicate that iron oxidation in Sample 2 was controlled by the localized temperature variation since Wustite forms preferably at higher temperatures. These subtle differences in the phase composition point to the sensitivity of the plasma spraying process toward even minor changes in operating conditions.

Sample 3: had a XRD pattern which reflected Al, $Fe_{0.9536}O$, Fe,Cr, $Fe^2Cr_2O_4$, Fe_3O_4 and Chromium as predominant phases in the composition. Thus, Cr occurrence in Sample 3 (Fig 6) not similarly the case with Sample 1 and Sample 2 signifies that deposition conditions in Sample 3 favored segregation of chromium. This could be due to variations in plasma spraying parameters, such as nozzle distance or cooling rates, which have taken effect on the crystallization of particular phases.

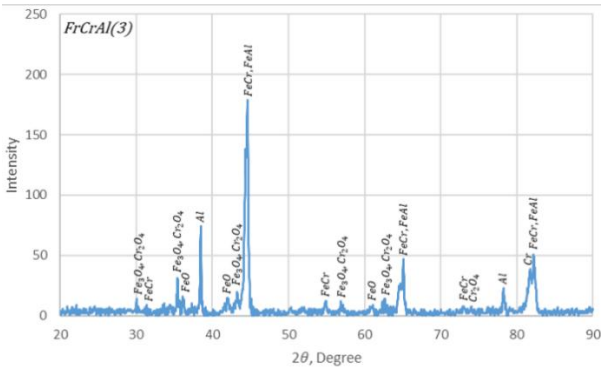


Fig. 6. XRD sample 03.

The detection of metallic chromium peaks would point out that the plasma jet has allowed the effect of localized cooling or shielding against excessive oxidation. The retention of Cr in its metallic state is definitely going to enhance corrosion resistance through building a self-healing oxide layer upon its exposure at high temperature. In relation to that, relatively weaker peaks about $Fe_{0.9536}O$ in comparison with those from $Fe^2Cr_2O_4$ support the assumption of probably slower or non-oxygen sufficient oxidation kinetics of iron within this sample. These features indicate that the deposition environment for Sample 3 had favorable conditions for chromium retention along with control of excessive iron oxidation.

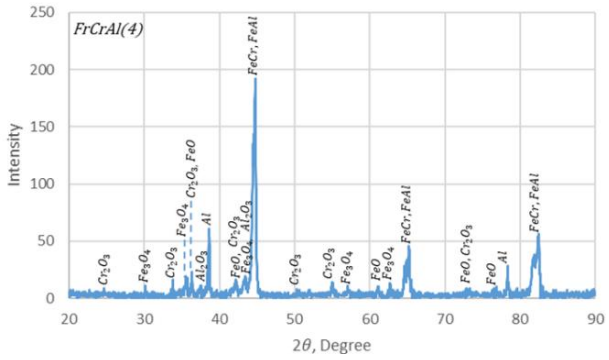


Fig. 7. XRD sample 04.

Sample 4: The XRD for Sample 4 (Fig 7) had peaks for Al, $Fe_{0.9536}O$, Fe,Cr, $Fe^2Cr_2O_4$, Fe_3O_4, Cr, Eskolaite Cr_2O_3, and Aluminium Oxide Al_2O_3. The further detection of Eskolaite and Aluminium Oxide in Sample 4 reflects a unique

phase formation likely due to distinct deposition or environmental conditions. The presence of Al_2O_3 + suggests partial oxidation of aluminium during the plasma spraying process, indicating that local temperature and oxygen availability were sufficient to oxidize the aluminium feedstock. Analogously, the formation of Cr_2O_3 indicates an advanced oxidation of chromium that could be attributed to prolonged exposure to high temperature and oxygen rich conditions. Coexistence of Cr and Cr_2O_3 suggests that while some regions allowed metallic chromium to remain intact, others facilitated its complete oxidation. These would then suggest that Sample 4 had deposition parameters involving higher local temperatures, more oxygen exposure, or longer cooling periods that resulted in a phase composition which is far more complex and rich in oxidation. Advanced oxidation for Sample 4 evidences its potential applications in stable oxide phases for improved wear and thermal resistance.

3.5 Coefficient of Friction

Coefficient of Friction: The frictional behaviour of FeCrAl samples was evaluated using a TRB3 Tribometer (Version 8.1.10) under controlled conditions to ensure reliable comparisons. Four FeCrAl samples (FeCrAl_1 to FeCrAl_4) were tested (Fig 8), maintaining consistent parameters, including a normal load of 4.00 N, linear sliding speed of 6.00 cm/s, and sliding radius of 3.00 mm. These settings ensured uniform sliding conditions and wear paths across all samples. Sample 1: Test result for Sample FeCrAl_1 was using laboratory temperature at 25.18 °C and relative humidity of 31.75%, normal load, 4.00 N sliding speed, and 6.00 cm/s sliding radius for 3.00 mm is imposed on a sample. That indicates interpreted as a fairly stable frictional response signifying reliable surface interaction which is practically the same throughout the test. These findings show that the coating and substrate properties were well matched, yielding a uniform tribological performance. Such stability is highly welcomed in applications requiring predictable wear rates and consistent frictional forces. Sample 02: Sample FeCrAl_2 was evaluated under slightly cooler and less humid conditions, with a laboratory temperature of 21.12 °C and a relative humidity of 22.97%. The CoF ranged from 0.043 to 0.889, with a mean value of 0.829 and a standard deviation of 0.093. The fact that the mean CoF obtained was higher when compared to the one obtained with FeCrAl_1 material reveals a surface interaction that should be more or less intense with either morphological changes in surfaces or the forming of oxide films upon sliding, possibly leading to increased adhesion or accumulation of wear debris due to higher frictional forces acting on the wearing surface. This sample will indicate the sensitivity of the tribological behaviour to surface conditions and microstructural features. Sample 03: Sample FeCrAl_3 was tested at the laboratory temperature of 21.77 °C and relative humidity of 21.83%. The friction coefficient ranged from 0.156 to 0.910. The average CoF was 0.841 with a standard deviation of 0.127. This had the largest standard deviation and thus the most variability in frictional behaviour. The higher CoF variability can, therefore, be related to localized variations in the surface roughness, adhesion, or tribo oxidation processes involved. Such heterogeneities may further indicate non uniform deposition or microstructural in homogeneities, which could enhance the effects of sliding contact on frictional behaviour. Sample 04: Sample FeCrAl_4 was tested at laboratory conditions of 22.61 °C with a relative humidity of 20.62%, while keeping test parameters identical. The friction co-efficient ranged from 0.145 to 0.929, with an average CoF of 0.864 and a standard deviation of 0.115. This sample had the highest average CoF out of the four samples, which could indicate more asperity interaction, more wear debris generation, or increased adhesive forces acting across the contacting surfaces.

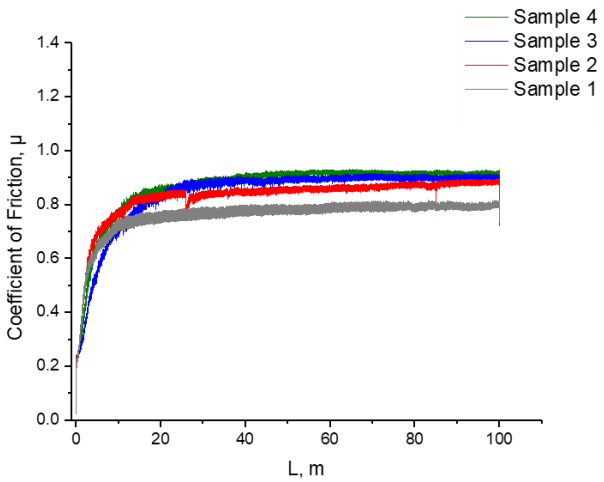


Fig. 8. CoF of FeCrAl samples.

3.6 Discussion

Discussion Coating Quality and Process Variability The coating thickness has varied from one sample to another, which shows the complexity of the plasma spraying process. These could be for several reasons: inconsistent spray parameters such as nozzle pressure, spray distance, and feedstock flow rate. Besides, substrate pre-heating, cooling rates after deposition, environmental conditions of temperature, and humidity add to these variations in coating thickness observed. Surface roughness analysis showed the trend that higher thicknesses normally had smoother surfaces. This would be because higher thickness is more uniform in deposition and has less number of defects. Smooth surfaces are better to provide high corrosion resistance and also wear resistance as there is minimal possibility for local failures. All the above variation in thickness and surface roughness did not have any effect on the hardness values of the sample. The final properties of the as deposited FeCrAl would then simply be independent from minor adjustments to coating thickness. The scattered variation in the values of hardness was quite encouraging as it suggests mechanical properties that would remain insensitive against moderate deposition parameters. Nevertheless, the friction coefficients, depicting the tribological behaviours for all these samples, reflected variability among these samples. The CoF values in some of the samples were higher, which might be due to increased surface asperities, adhesive forces, or wear debris generation during sliding. These results highlight the need for better control of deposition parameters in order to reduce variability and to achieve improved coating performance. Better standardization of the plasma spraying process, along with the refinement of substrate preparation methods, could substantially improve coating uniformity and its tribological performance.

4. CONCLUSION

Underlines the challenges and opportunities that exist towards optimizing FeCrAl coatings deposition processes. Variability in the thickness of coatings was identified as one of the major challenges, highly affecting surface roughness and tribological performance. Thicker coatings generally yielded smoother surfaces; thus, deposition uniformity can enhance the functional properties of the coatings. It also showed that hardness remained constant for all samples, which means that mechanical properties are independent of coating thickness. However, regarding tribological performance, represented by the coefficient of friction, sample dependent variability was recorded. These differences point out the sensitivity of frictional behaviour to surface characteristics and microstructural features. Future work should give priority to the refinement of plasma spraying parameters in order to achieve consistent coating thickness and improved surface finish. Further work on improved substrate preparation and in situ monitoring during deposition will lead to further reduction in variability. In additionally, the investigation of the dependence of coating thickness on other properties, such as wear resistance and corrosion resistance, will lead to more fundamental understanding in the performance of the FeCrAl coatings in industrial applications. These will eventually contribute to the creation of more reliable and durable coatings in the harsh environments, (Table 1).

Acknowledgement

This research has been funded by the Science Committee of the Ministry of Education and Science of the Republic of Kazakhstan (Grant No. BR24992862).

REFERENCES

[1] V. Boronenkov and Y. Korobov, Fundamentals of Arc Spraying: Physical and Chemical Regularities. Berlin, Germany: Springer, 2016.

[2] J. Lee, H. Kwon, Y. G. Kim, and C. Lee, "Tribological and microstructural properties of carbon steel coatings fabricated by wire arc spray," Metals Mater. Int., vol. 26, no. 5, pp. 650–659, May 2020.

[3] S. Samal, "Thermal plasma technology: The prospective future in material processing," J. Cleaner Prod., vol. 142, pp. 3131–3150, Jan. 2017.

[4] R. M. Castro, L. C. C. Cavaler, F. M. Marques, V. M. Bristot, and A. S. Rocha, "Comparative of the tribological performance of hydraulic cylinders coated by the process of thermal spray HVOF and hard chrome plating," Tribol. Ind., vol. 36, no. 1, pp. 79–89, Mar. 2014.

[5] N. Babu, R. Balasubramaniam, and A. Ghosh, "High-temperature oxidation of Fe3Al-based iron aluminides in oxygen," Corros. Sci., vol. 43, no. 12, pp. 2239–2254, Dec. 2001, doi: 10.1016/S0010-938X(01)00036-3.

[6] T. Yamashita and P. Hayes, "Analysis of XPS spectra of Fe2+ and Fe3+ ions in oxide materials," Appl. Surf. Sci., vol. 254, no. 8, pp. 2441–2449, Feb. 2008, doi: 10.1016/j.apsusc.2007.09.063.

[7] C. R. Brundle, T. J. Chuang, and K. Wandelt, "Core and valence level photoemission studies of iron oxide surfaces and the oxidation of iron," Surf. Sci., vol. 68, pp. 459–468, Nov. 1977.

[8] C. Q. Cheng, J. Zhao, T. S. Cao, Q. Q. Fu, and M. K. Lei, "Facile chromaticity approach for the inspection of passive films on austenitic stainless steel," Corros. Sci., vol. 70, pp. 235–242, May 2013.

[9] X. Liu et al., "Using high-temperature mechanochemistry treatment to modify iron oxide and improve the corrosion performance of epoxy coating–I. High-temperature ball milling treatment," Corros. Sci., vol. 90, pp. 451–462, Jan. 2015.

[10] Y. Gao and S. A. Chambers, "Heteroepitaxial growth of α-Fe2O3, γ-Fe2O3 and Fe3O4 thin films by oxygen-plasma-assisted molecular beam epitaxy," J. Cryst. Growth, vol. 174, no. 1–4, pp. 446–454, Apr. 1997.

[11] H. Hu et al., "Study of the corrosion behavior of a 18Cr-oxide dispersion strengthened steel in supercritical water," Corros. Sci., vol. 65, pp. 209–213, Dec. 2012.

[12] J. Yuan, W. Wang, S. Zhu, and F. Wang, "Comparison between the oxidation of iron in oxygen and in steam at 650–750°C," Corros. Sci., vol. 75, pp. 309–317, Oct. 2013, doi: 10.1016/j.corsci.2013.06.009.

[13] L. Liu et al., "Effect of water vapour on the oxidation of Fe–13Cr–5Ni martensitic alloy at 973 K," Corros. Sci., vol. 60, pp. 90–97, Jul. 2012.

[14] W. Zhang et al., "Screening of the FeCrAl LBE corrosion-resistant coatings: The effect of Cr and Al contents," Surf. Coat. Technol., vol. 462, p. 129477, Jun. 2023, doi: 10.1016/j.surfcoat.2023.129477.

[15] L. Zhou et al., "Plasma sprayed Al2O3/FeCrAl composite coatings for electromagnetic wave absorption application," Appl. Surf. Sci., vol. 258, no. 7, pp. 2691–2696, Jan. 2012.

[16] L. Pawlowski, The Science and Engineering of Thermal Spray Coatings, 2nd ed. Chichester, U.K.: Wiley, 2008.

[17] A. Kengesbekov, "Influence of plasma arc current and gas flow on the structural and tribological properties of TiN coatings obtained by plasma spraying," Coatings, vol. 14, no. 11, p. 1404, Nov. 2024, doi: 10.3390/coatings14111404.

[18] A. D. Pogrebnjak et al., "The effects of Cr and Si additions and deposition conditions on the structure and properties of the (Zr-Ti-Nb)N coatings," Ceram. Int., vol. 43, no. 1, pp. 771–782, Jan. 2017.

[19] A. Mamaeva et al., "Influence of current duty cycle and voltage of micro-arc oxidation on the microstructure and composition of calcium phosphate coating," Coatings, vol. 14, no. 6, p. 766, Jun. 2024, doi: 10.3390/coatings14060766.

[20] A. M. Yermakhanova, A. K. Kenzhegulov, M. N. Meiirbekov, and B. M. Baiserikov, "Comparative study of dielectric characteristics and radio transparency of composite materials," J. Elastomers Plast., vol. 56, no. 7, pp. 843–857, Nov. 2024.

[21] A. T. Ospanali et al., "Obtaining of carbon nanofibers based on polyacrylonitrile by the method of electrospinning," Eurasian Phys. Tech. J., vol. 33, no. 1, pp. 35–38, 2020.

[22] A. Kengesbekov et al., "Synthesis and formation mechanism of metal oxide compounds," Coatings, vol. 12, no. 10, p. 1511, Oct. 2022, doi: 10.3390/coatings12101511.

[23] B. K. Rakhadilov, L. G. Zhurerova, Z. B. Sagdoldina, A. B. Kenesbekov, and L. B. Bayatanova, "Morphological changes in the dislocation structure of structural steel 20GL after electrolytic-plasma hardening of the surface," J. Surf. Investig.: X-ray, Synchrotron Neutron Tech., vol. 15, no. 2, pp. 408–413, Mar. 2021.

[24] B. Rakhadilov et al., "Impact of electronic radiation on the morphology of the fine structure of the surface layer of R6M5 steel," Machines, vol. 9, no. 2, p. 24, Jan. 2021, doi: 10.3390/machines9020024.